# Ternary Inulin Hydrogel with Long-Term Intestinal Retention for Simultaneously Reversing IBD and its Fibrotic Complication

Xiangjing Cao[1], Shi Tao[1], Weitao Wang[1], Silong Wu[2], Yang Hong[1], Xuyuan Wang[2], Yan Ma[2, 3*], Haisheng Qian[2*], Zhengbao Zha[1*]

[1]School of Food and Biological Engineering, Hefei University of Technology, Hefei 230009, China.

[2]School of Biomedical Engineering, Anhui Medical University, Hefei 230022, China.

[3]Key Laboratory of Science and Engineering for the Multi-modal Prevention and Control of Major Chronic Diseases, Ministry of Industry and Information Technology, Harbin Institute of Technology Zhengzhou Research Institute, Zhengzhou, 450000, China

[*]Corresponding author. Email: may@ahmu.edu.cn (Y.M.); shqian@ahmu.edu.cn (H.Q.); zbzha@hfut.edu.cn (Z.Z.)

## Supplementary Figures

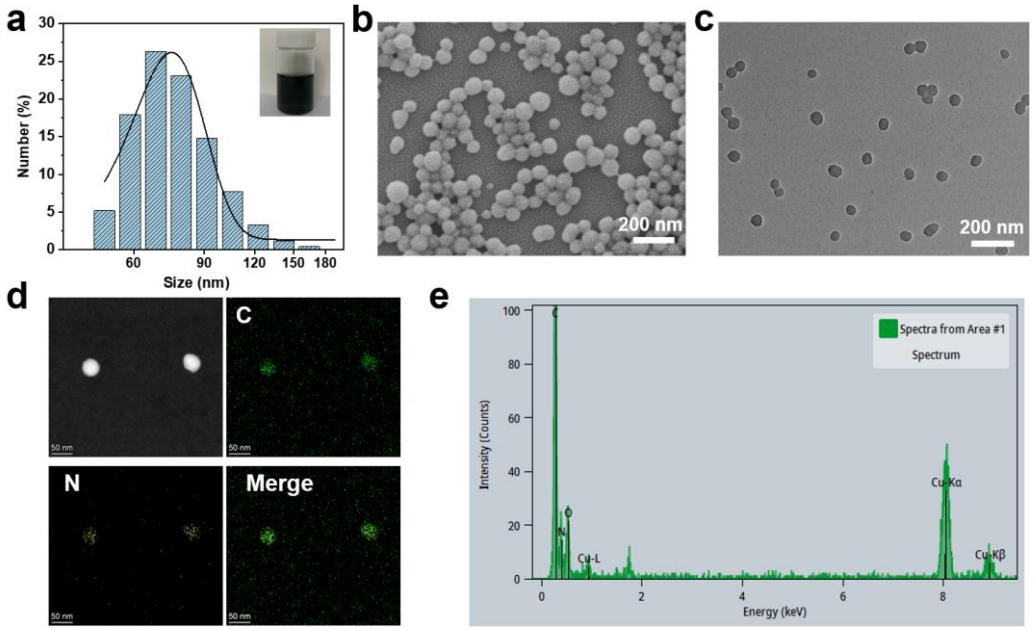


**Supplementary Fig. 1. a** DLS, (**b**) SEM, and (**c**) TEM images of PPy nanozymes. DLS, TEM, and SEM analyses revealed that PPy nanozymes exhibited a relatively uniform spherical morphology, with particle size predominantly distributed in the range of 60 to 80 nm. **d** Element maps of PPy nanozymes; **e** The energy dispersive spectrometer mapping of PPy nanozymes. In **b-d**, the representative SEM and TEM images are shown (at least three images were taken for each sample).

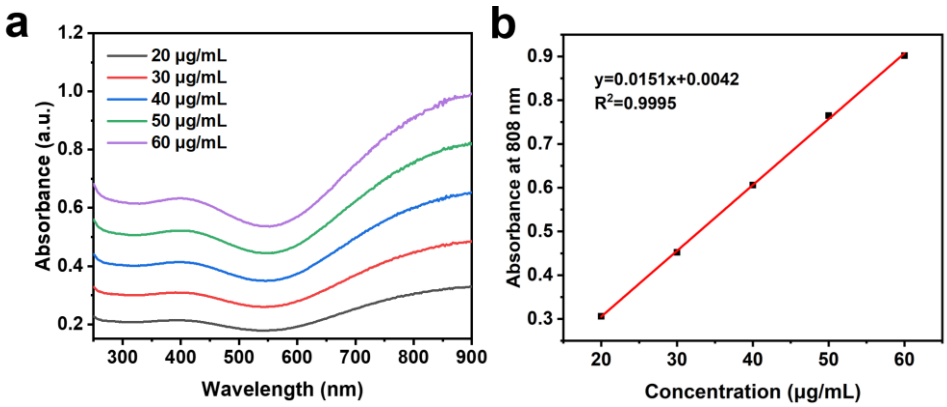


**Supplementary Fig. 2. a** UV-vis-NIR absorption spectra of PPy nanozymes at different concentrations. **b** The absorbance at 808 nm as a function of the concentration of the PPy nanozymes. PPy nanozymes shows strong absorption in near infrared regions, and absorption at 808 nm is linearly related to its concentration.

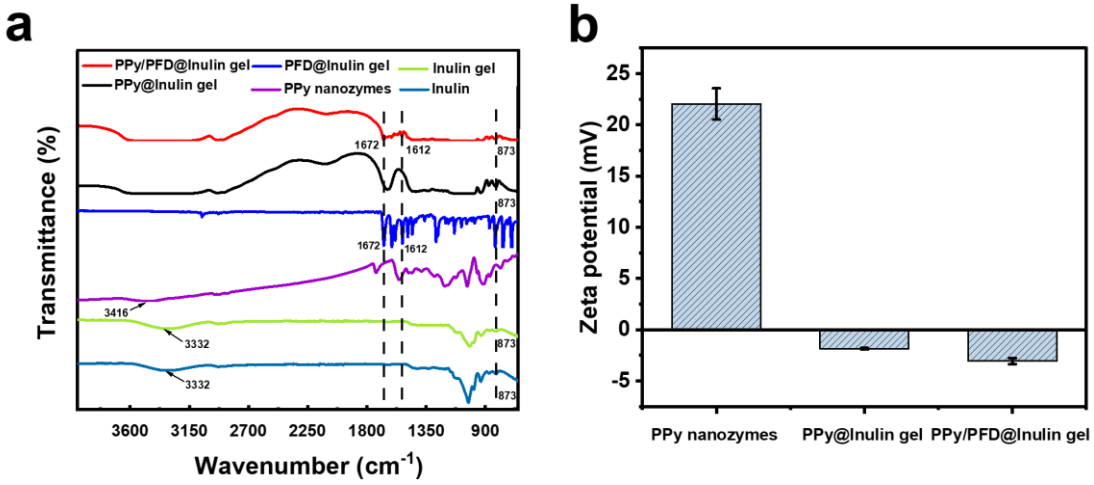


**Supplementary Fig. 3. a** Fourier transform infrared (FTIR) spectrum and (**b**) Zeta potential before and after PPy/PFD@Inulin gel. The peak at 873 $cm^{-1}$ corresponds to the transverse methylene vibration of the furanose molecule in inulin. The peak at 1672 $cm^{-1}$ is the characteristic absorption peak of the pyridine ring C=O in PFD, while the peak at 1612 $cm^{-1}$ represents the characteristic absorption of the C-N pyridine ring in PFD. Furthermore, the absorption peak at 3332 $cm^{-1}$ is attributed to the stretching vibration absorption of -OH in the inulin molecule, and the peak at 3416 $cm^{-1}$ corresponds to the stretching vibration of the pyrrole ring. Both -OH and -NH groups are present in PPy@Inulin gel and PPy/PFD@Inulin gel, resulting in broadening of the peak in the range of 3600 to 3000 $cm^{-1}$.

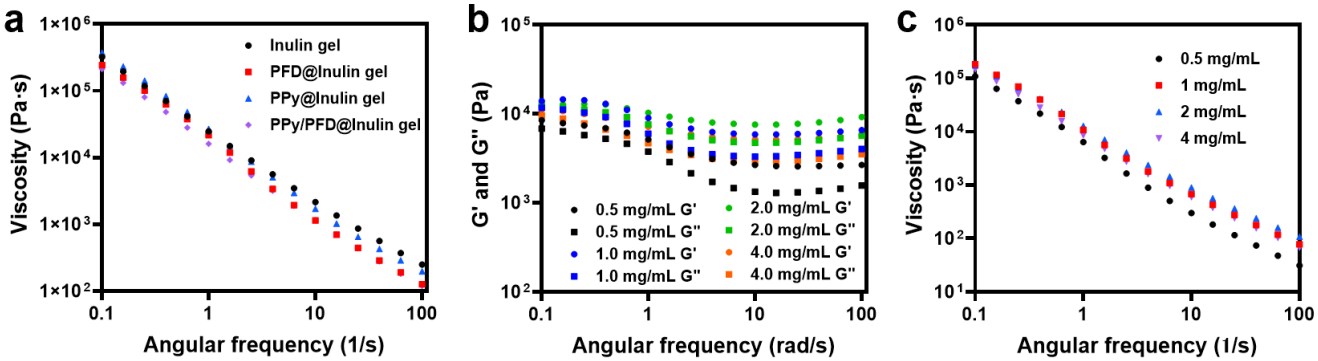


**Supplementary Fig. 4. a** Viscosity measurements of four different gels by dynamic rheological tests. Dynamic rheological tests of PPy/PFD@Inulin gel with different concentrations of PPy nanozymes. Frequency amplitude sweep curves (**b**) and viscosity test (**c**).

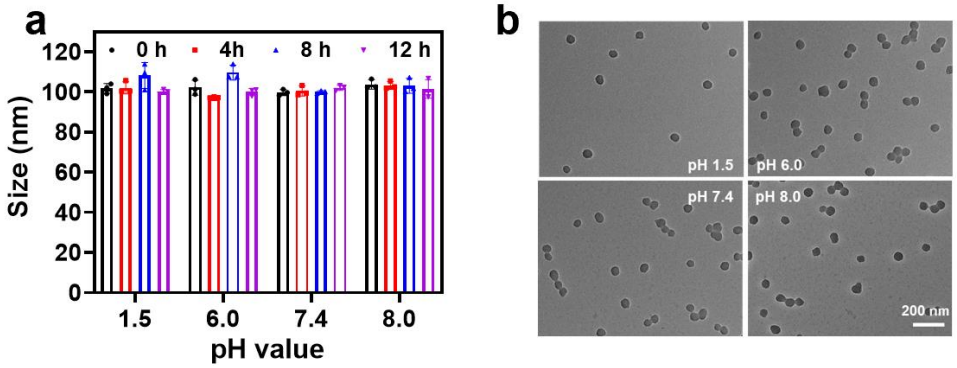


**Supplementary Fig. 5. a** The size of PPy nanozymes after treating for 0, 4, 8, and 12 h in pH 1.5, pH 6.0, pH 7.4, pH 8.0 solution. **b** The TEM image of PPy nanozymes after treating for 6 h in pH 1.5, pH 6.0, pH 7.4, pH 8.0 solution. Data are presented as mean ± SD (n = 3 biologically independent samples for (**a**)). In **b**, the representative TEM images are shown (at least three images were taken for each sample).

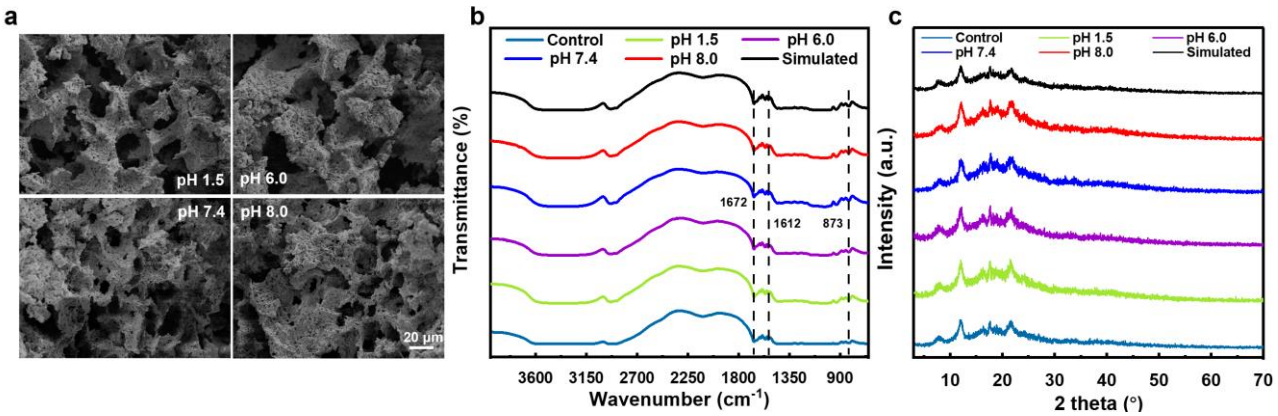


**Supplementary Fig. 6. a** The SEM image of PPy/PFD@Inulin gel after treating for 6 h in pH 1.5, pH 6.0, pH 7.4, pH 8.0 solution. **b** FTIR and XRD (**c**) of PPy/PFD@Inulin gel after simulated treatment in different pH PBS and simulated Gastrointestinal Environment. In **a**, the representative SEM images are shown (at least three images were taken for each sample).

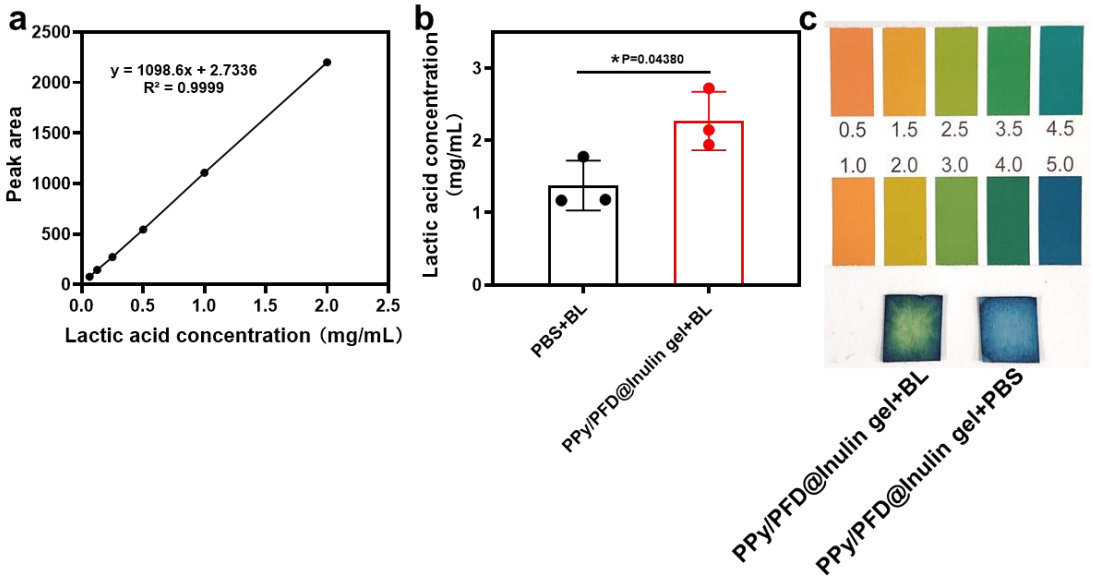


**Supplementary Fig. 7. a** The relationship between different concentrations of lactic acid and peak area was determined by high performance liquid chromatography. **b** Lactic acid concentration of PPy/PFD@Inulin gel in PBS and BL. **c** Degradation of PPy/PFD@Inulin gel in PBS and BL, pH in upper liquid. Data are presented as mean ± SD (n = 3 biologically independent samples for (**b**)). Statistical analysis was evaluated with two-tailed Student's t tests. $p > 0.05$ (n.s.), $*p < 0.05$, $**p < 0.01$, $***p < 0.001$.

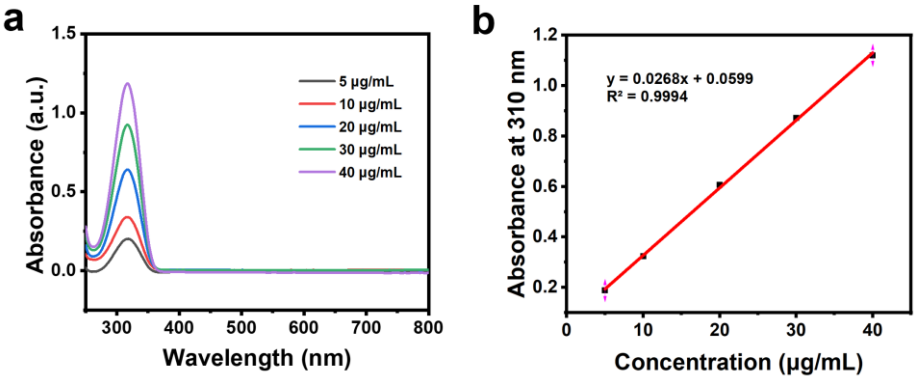


**Supplementary Fig. 8. a** UV absorption spectra of PFD at different concentrations. **b** The absorbance at 310 nm as a function of the concentration of the PFD. PFD exhibited strong absorption at 318 nm, and a robust linear relationship between absorption and concentration was observed.

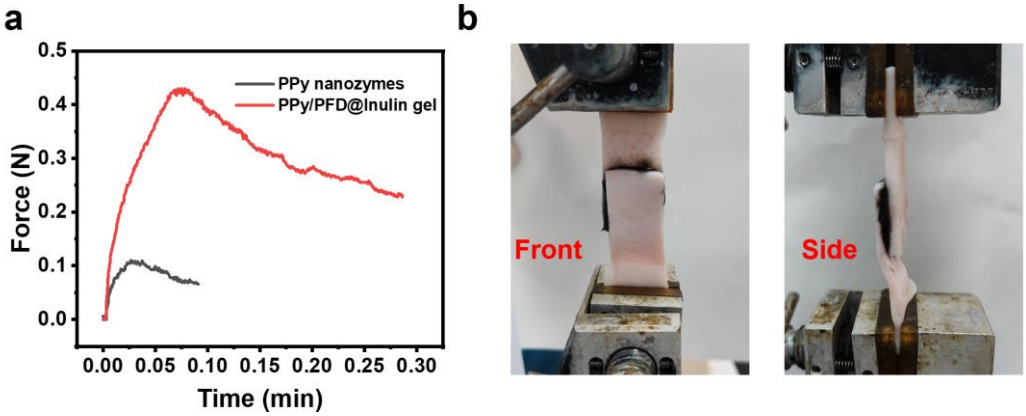


**Supplementary Fig. 9. a** The adhesion forces of PPy/PFD@Inulin gel and PPy nanozymes. **b** The photo of the lap-shear test to measure the adhesive energy.

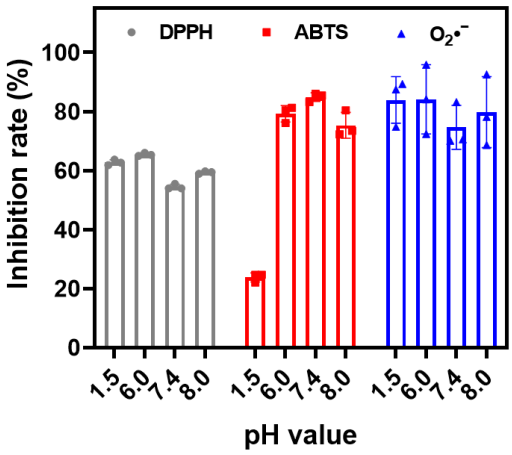


**Supplementary Fig. 10.** At different pH (pH=1.5, 6.0, 7.4, 8.0), the inhibition rates of DPPH, ABTS and $O_2^{\cdot -}$ were determined. Data are presented as mean ± SD (n = 3 biologically independent samples).

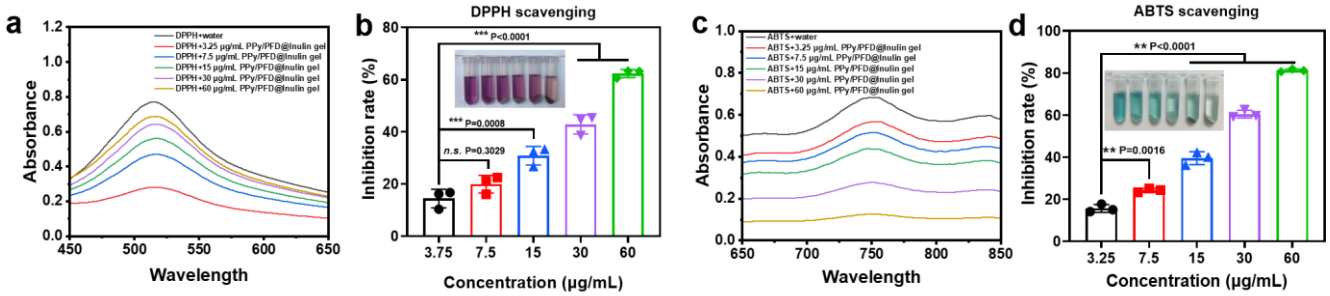


**Supplementary Fig. 11. a** The UV−Vis spectra of PPy/PFD@Inulin gel after reaction with DPPH in the presence of different concentrations of PPy nanozymes. **b** The dependence of the elimination rate of DPPH on the concentration of PPy nanozymes. **c** The UV−Vis spectra of PPy/PFD@Inulin gel after reaction with ABTS in the presence of different concentrations of PPy nanozymes. **d** The dependence of the elimination rate of ABTS on the concentration of PPy nanozymes. Data are presented as mean ± SD (n = 3 biologically independent samples for (**b** and **d**)). Statistical analysis was performed using one-way ANOVA. P > 0.05 (n.s.), *p < 0.05, **p < 0.01, ***p < 0.001.

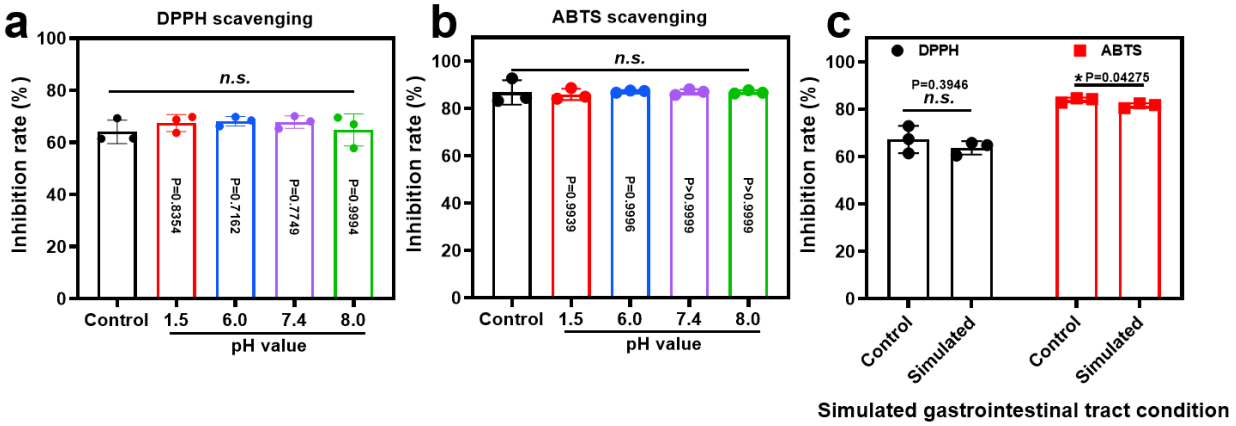


**Supplementary Fig. 12. a** At different pH levels (pH 1.5, 6.0, 7.4, and 8.0), the inhibition rates of DPPH and ABTS (**b**) by PPy/PFD@Inulin gel were determined. **c** After simulating the gastrointestinal environment, PPy/PFD@Inulin gel was used to determine its clearance rate of DPPH and ABTS. Data are presented as mean ± SD (n = 3 biologically independent samples). Statistical analysis was performed using one-way ANOVA (**a** and **b**), statistical analysis was evaluated with two-tailed Student's t tests (**c**). P > 0.05 (n.s.), *p < 0.05, **p < 0.01, ***p < 0.001.

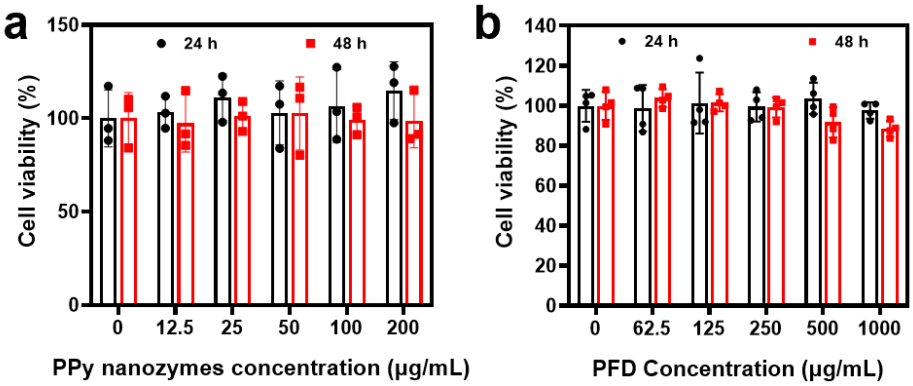


**Supplementary Fig. 13. a** NCM460 cells viability after incubated with various concentrations of PPy nanozymes for 24 or 48 h. **b** NCM460 cells viability after incubated with various concentrations of PFD for 24 or 48 h. Data are presented as mean ± SD (n = 3 biologically independent samples for (**a**), n = 4 biologically independent samples for (**b**)).

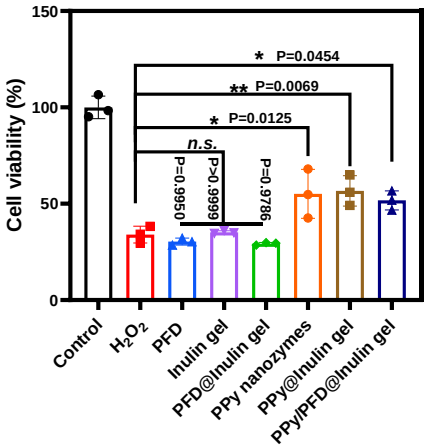


**Supplementary Fig. 14.** In the presence of 1mM $H_2O_2$, the cell viability of different groups of materials was tested. Data are presented as mean ± SD (n = 3 biologically independent samples). Statistical analysis was performed using one-way ANOVA. P > 0.05 (n.s.), *p < 0.05, **p < 0.01, ***p < 0.001.

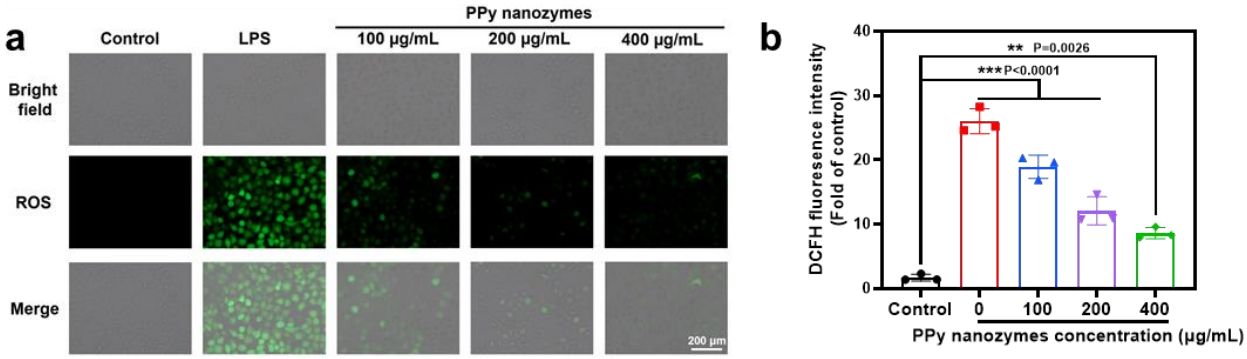


**Supplementary Fig. 15. a** PPy nanozymes inhibition of intracellular ROS production in 800 ng/mL LPS-treated NCM460 cells stained with DCFH-DA. **b** The corresponding mean fluorescence intensity. Data are presented as mean ± SD (n = 3 biologically independent samples). Images from one representative experiment of three independent experiments are presented. Statistical analysis was performed using one-way ANOVA. P > 0.05 (n.s.), *p < 0.05, **p < 0.01, ***p < 0.001.

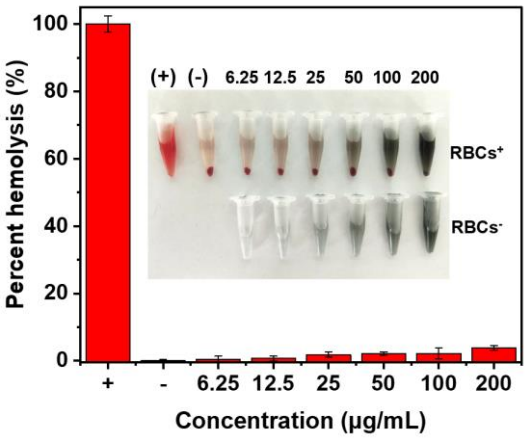


**Supplementary Fig. 16.** The percentage of red blood cell (RBC) haemolysis was assessed in the presence of different concentrations of PPy nanozymes. Data are presented as mean ± SD (n = 3 biologically independent samples).

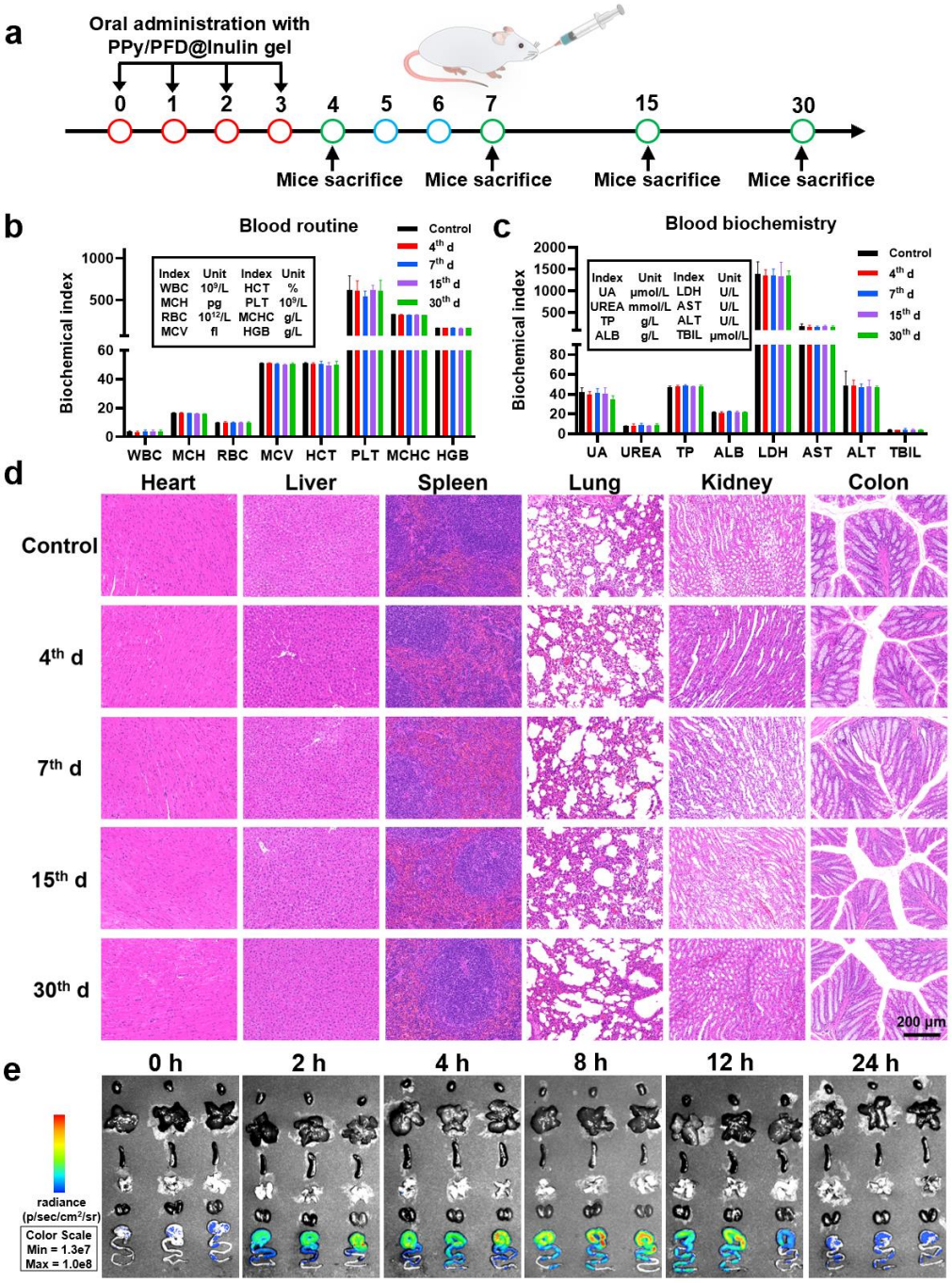


**Supplementary Fig. 17.** Biocompatibility and biodistribution of PPy/PFD@Inulin gel. **a** Schematic illustration for biocompatibility assessment. **b** Blood routine and **(c)** blood biochemistry indexes. **d** H&E staining of various organsimages. **e** *In vitro* biodistribution fluorescent images of oral Cy5.5-PPy/PFD@Inulin gel in major organs (n=3 biologically independent samples). Data are presented as mean ± SD (n=3 biologically independent samples for (**b** and **c**)). The representative images in **d** are shown from three independent mice.

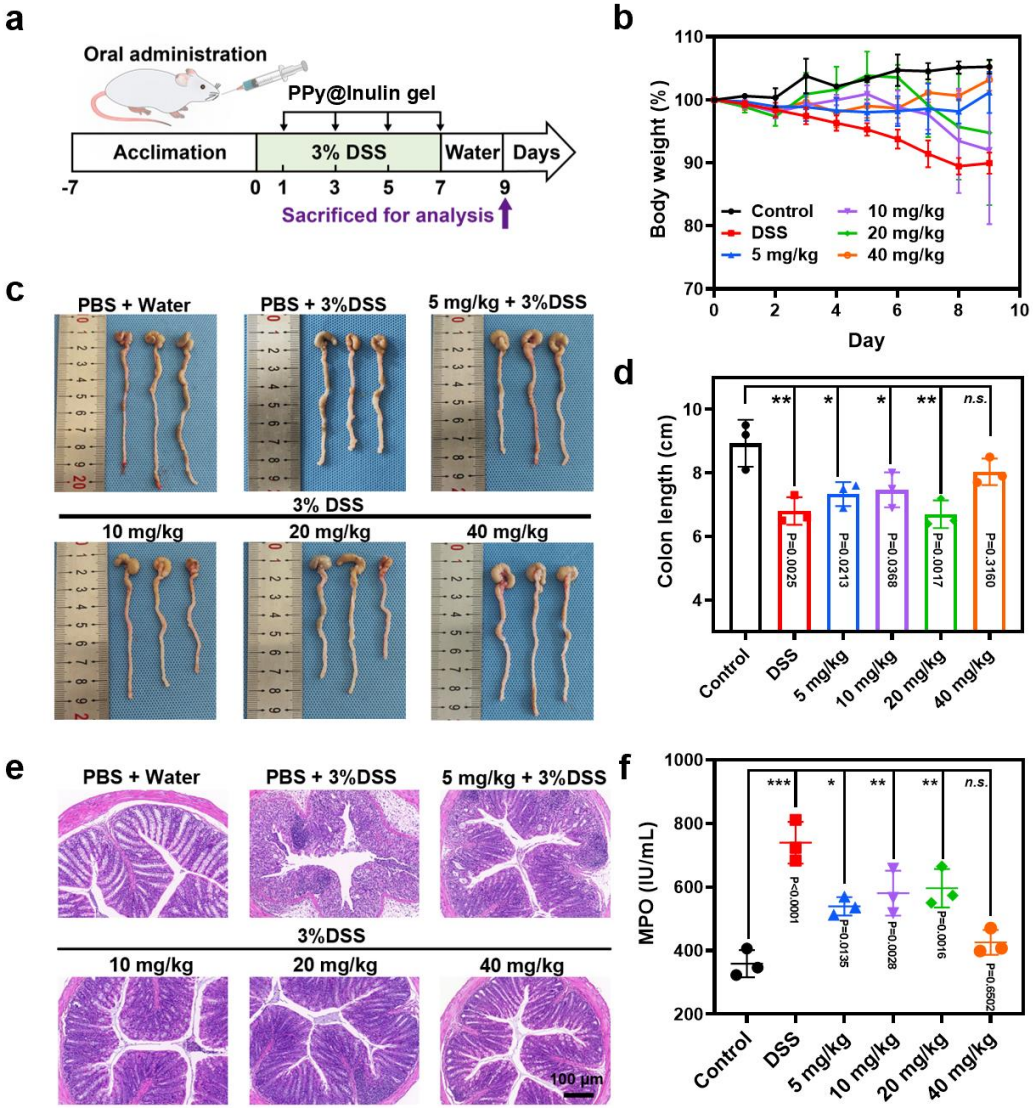


**Supplementary Fig. 18.** Explore the appropriate dose to treat IBD. **a** Experimental design of DSS induced IBD model mice. The mice were given drinking water or 3% DSS water for 7 days. Oral administration on days 1, 3, 5 and 7. The mice were killed 2 days after DSS was discontinued. **b** Daily changes of body weight were recorded in detail every day. **c** Digital photos of the colons of each group of mice on day 9. **d** Colon length of mice with indicated treatment on day 9. **e** H&E staining of representative mouse colon tissue. The scale bar is 100 μm. **f** MPO activity in the supernatant after homogenization of mouse colon tissue. Data are presented as mean ± SD (n = 3 biologically independent samples for (**b**, **d**, and **f**)). The representative images in **e** are shown from three independent mice. Statistical analysis was performed using one-way ANOVA. $P > 0.05$ (n.s.), $^{*}p < 0.05$, $^{**}p < 0.01$, $^{***}p < 0.001$.

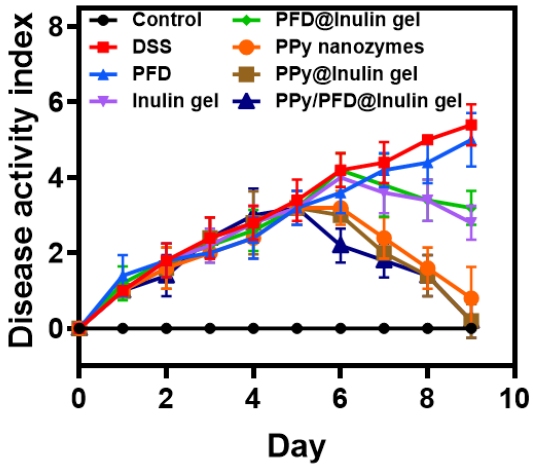


**Supplementary Fig. 19.** DAI scores of different groups of mice over 9 days. Data are presented as mean ± SD (n = 5 biologically independent samples).

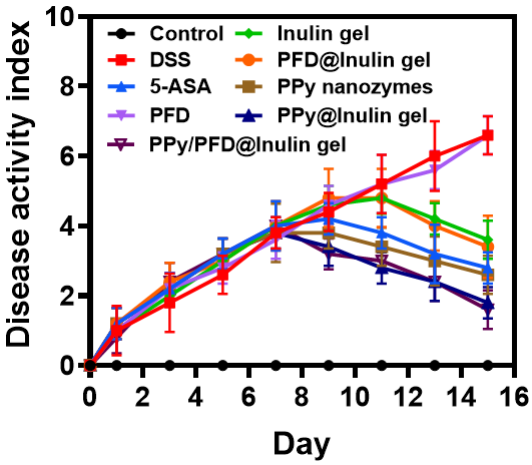


**Supplementary Fig. 20.** DAI scores of different groups of mice over 15 days. Data are presented as mean ± SD (n = 5 biologically independent samples).

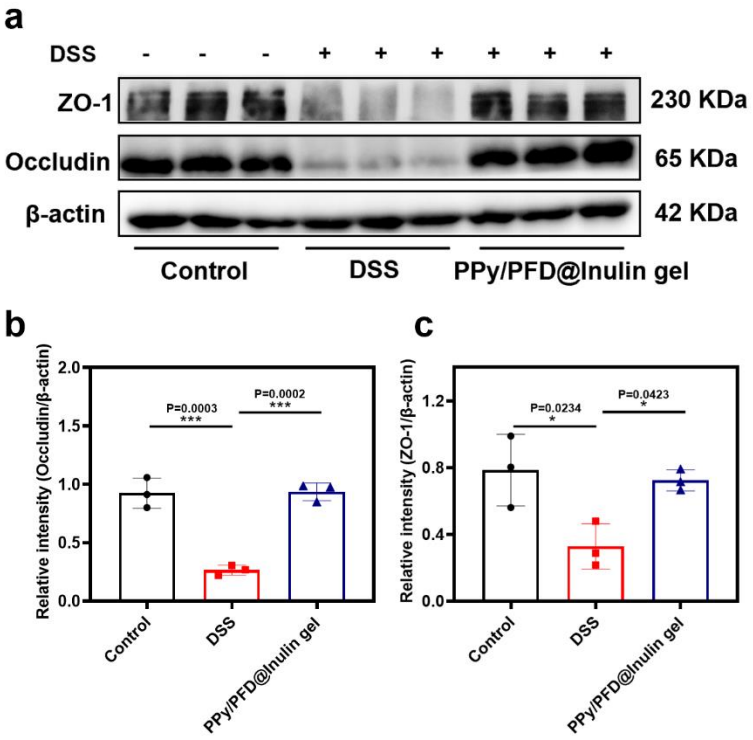


**Supplementary Fig. 21. a** Western blotting analysis of Occludin and ZO-1 expression of protein extracts from colon tissue. **b, c** Quantitative Western blot analyses were performed. Statistical analysis was performed using one-way ANOVA. P > 0.05 (n.s.), *p < 0.05, **p < 0.01, ***p < 0.001.

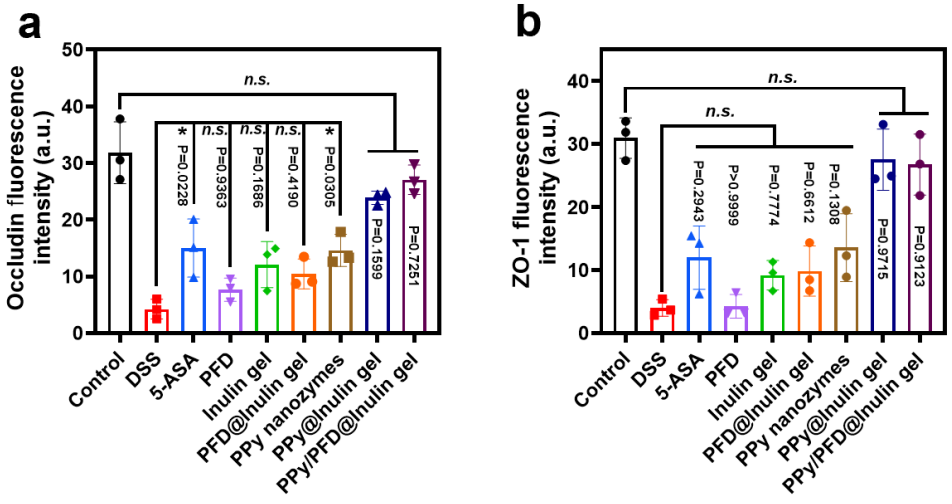


**Supplementary Fig. 22.** The relative fluorescence intensity of Occludin (a) and ZO-1 (b) proteins in colon. Data are presented as mean ± SD (n = 3 biologically independent samples). Statistical analysis was performed using one-way ANOVA. P > 0.05 (n.s.), *p < 0.05, **p < 0.01, ***p < 0.001.

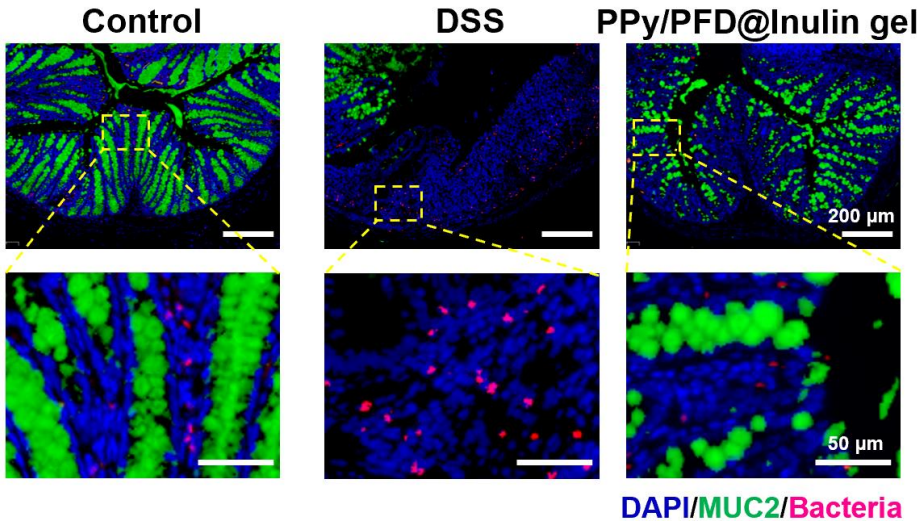


**Supplementary Fig. 23.** FISH (EUB338) combined with immunofluorescence imaging (anti-Muc2 antibody) analysis of the colon sections. The representative images are shown from three independent mice.

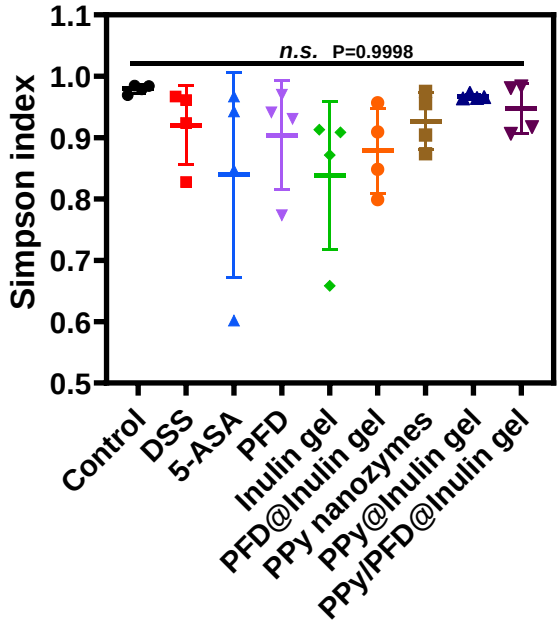


**Supplementary Fig. 24.** Estimation of the gut microbial richness by the number of indices of community α-diversity determined by Simpson. Data are presented as mean ± SD (n = 4 biologically independent samples). Statistical analysis was evaluated with two-tailed Student's t tests. $p > 0.05$ (n.s.), $*p < 0.05$, $**p < 0.01$, $***p < 0.001$.

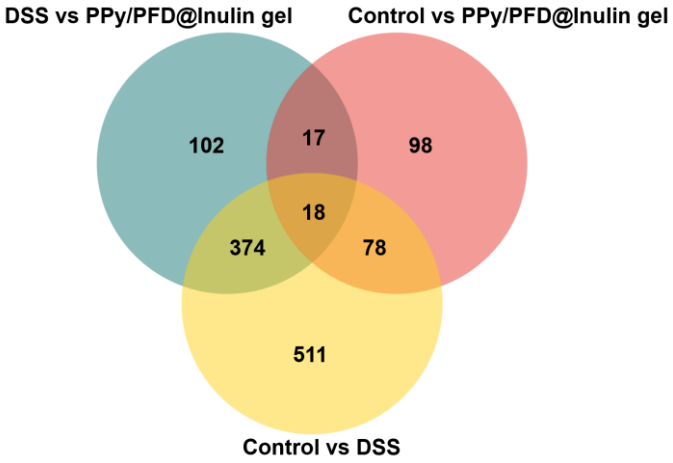


**Supplementary Fig. 25.** Venn diagram of colonic DEGs among three groups of Controls, DSS groups, and PPy/PFD@Inulin gel groups (n = 4 biologically independent samples).

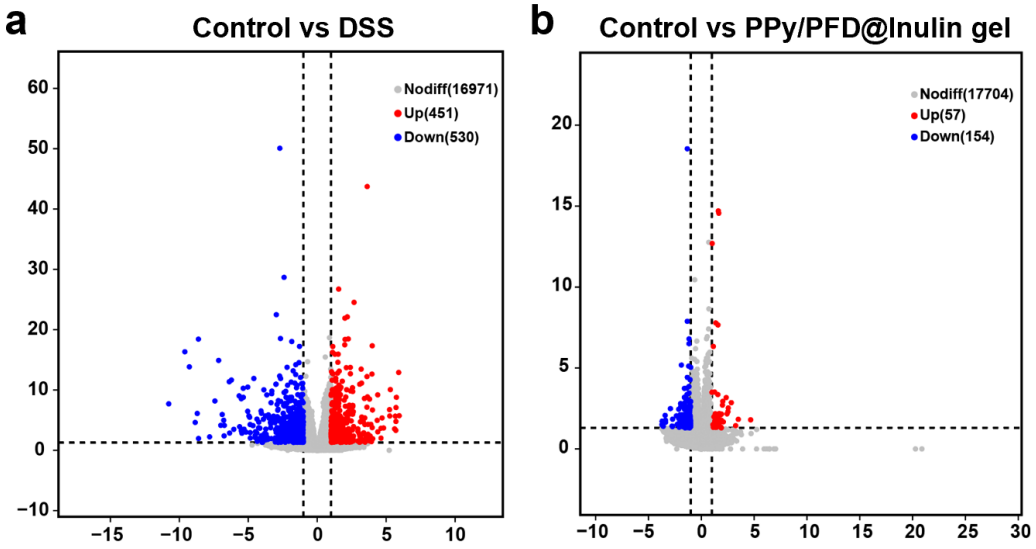


**Supplementary Fig. 26.** Volcano plots of DEGs was identified when comparing Control vs DSS and Control vs PPy/PFD@Inulin gel, with each point corresponding to an individual gene. Red and blue points denote upregulated and downregulated genes, respectively, while non-significant genes are shown in grey (n = 4 biologically independent samples).

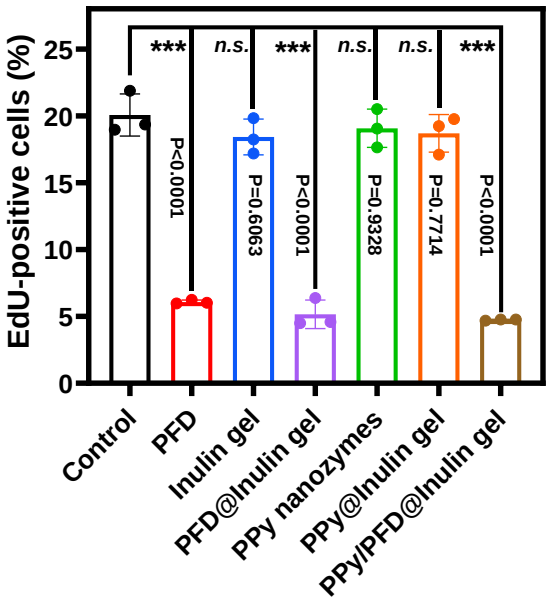


**Supplementary Fig. 27.** Quantification of EdU positive cells in the EdU test (n = 3 biologically independent samples). Statistical analysis was performed using one-way ANOVA. P > 0.05 (n.s.), *p < 0.05, **p < 0.01, ***p < 0.001.

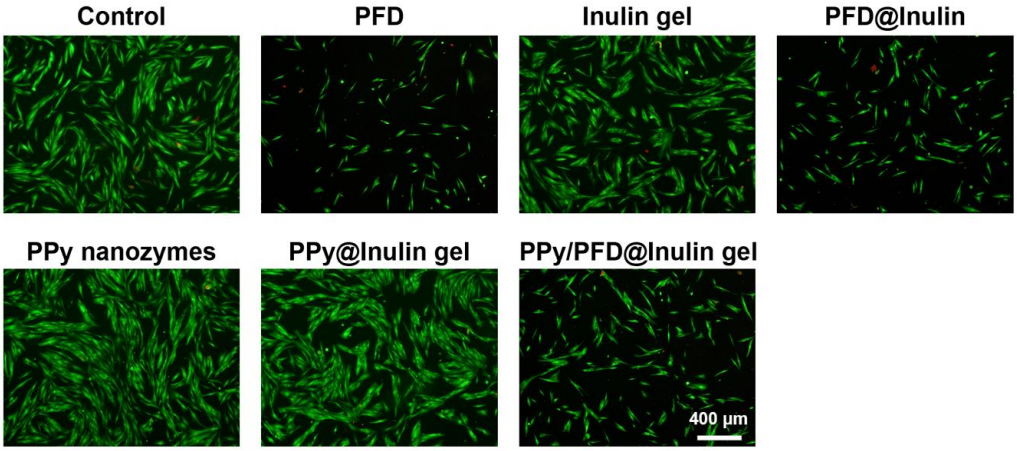


**Supplementary Fig. 28.** The fluorescent images of CCD-18Co cells co-stained with calcein-AM/PI after different groups of materials were incubated with CCD-18Co cells for 48 h. The scale bar is 400 μm. Images from one representative experiment of three independent experiments are presented.